

Size-selective two-photon spectroscopy of CuCl spherical quantum dots

A. V. Baranov* and Y. Masumoto

Institute of Physics, University of Tsukuba, Tsukuba, Ibaraki 305, Japan

K. Inoue

Research Institute for Electronic Science, Hokkaido University, Sapporo, 060, Japan

A. V. Fedorov and A. A. Onushchenko

S. I. Vavilov State Optical Institute, 199034 St. Petersburg, Russia

(Received 13 January 1997; revised manuscript received 28 February 1997)

We analyze luminescence spectra resulting from a resonant size-selective two-photon excitation of the low-energy confined Z_3 -exciton states in CuCl spherical nanocrystals. Excitation spectra of the two-photon-excited luminescence (TPL) bands and size dependences of band energies show that the TPL bands arise due to annihilation of the exciton in the lowest-energy state excited both directly and through the higher-energy confined states. It is shown that the observed features of the TPL fine structure can be unambiguously interpreted in terms of longitudinal (L) and transverse (T) confined exciton states and resonant enhancement of phonon-assisted luminescence when the energy gap between $1S$ and $1P$ states of the T exciton is close to the LO-phonon energy. [S0163-1829(97)03024-5]

I. INTRODUCTION

Three-dimensional confinement results in a drastic change of the electronic structure of semiconductor nanocrystals or quantum dots (QD's) if their size approaches the exciton Bohr radius of the corresponding bulk crystal. The confinement effects on the low-energy electron-hole pair states are usually most pronounced and allow an unambiguous interpretation of experimental data. In fact, several studies have led to the discovery of fine details of the confinement effect. Recently, an analysis of the luminescence spectra at one-photon excitation in the region of $1S$ and $1P$ confined Z_3 -exciton states of CuCl nanocrystals embedded in a glass matrix has provided evidence for excitonic polaron and exciton-phonon complexes with size-dependent behaviors.¹ The multiphonon structure of the two-photon excited luminescence (TPL) of CuBr QD's at two-photon excitation in the vicinity of the lowest-energy $1S$ confined $Z_{1,2}$ -exciton state shows that strongly coupled exciton-LO-phonon states, similar in some sense to molecular vibronic states, appear in semiconductor QD's.² Theoretically predicted enhancement of the short-range exchange interaction in QD's (Ref. 3) by quantum confinement has been experimentally observed for CdSe quantum dots by polarized luminescence studies⁴ and by a magnetic-field dependence of luminescence spectra and decay.⁵ In the latter case the strongly enhanced exchange interaction is claimed to allow the observation of a triplet exciton.

Of great interest is the long-range exchange interaction in QD's. It is well known that in bulk crystals this interaction is responsible for the splitting of the Wannier exciton into longitudinal (L) and transverse (T) branches,⁶ which yields the L - T exciton splitting energy gap Δ_{LT} . An attempt to theoretically consider the contribution of the long-range exchange interaction to the splitting energies in QD's has been

made in Ref. 3 and the result has been used for analysis of luminescence spectra of CdSe QD's.⁷ However, the L - T splitting in QD's has not been observed yet and is still an open question. Since two-photon generation of the longitudinal exciton is possible,⁸ it is expected to be manifested in TPL spectra of QD's.

The study reported in this paper was performed on CuCl semiconductor nanocrystals of spherical shape embedded in a glass matrix. The CuCl nanocrystals provide a typical example in the weak confinement regime. Secondary emission spectra have been analyzed when the samples are two-photon excited in the region of low-energy confined states of the Z_3 exciton. This choice has been made mainly for the following reasons. First, QD's of cubic semiconductors of T_d symmetry allow a more adequate theoretical description of the confinement effects than, for example, QD's of hexagonal semiconductors. Second, the lowest-energy exciton state in CuCl is the spin-orbit split-off Z_3 -exciton one and the spin-orbit splitting energy $\Delta_{so} = 93.4$ meV is large enough to neglect mixing between the spin-orbit split-off exciton and the heavy (light) exciton. Third, in the weak confinement regime, as has been verified,^{9,10} the size dependence of the lowest-energy confined Z_3 -exciton state $1S$ satisfies the relation $E_{1S} = \hbar^2 \pi^2 / 2MR^2$, where M is the translational mass of the exciton ($M = 2.3m_0$, with m_0 being the free-electron mass) and R is the radius of the QD. Hence it is reasonable to suppose that the size dependence of the $1P$ state energy will also be described by the same expression with π replaced by 4.49 .¹¹ Fourth, the two-photon spectroscopy has already been shown to provide a promising size-selective spectroscopic method for quantum dot systems^{2,12-14} because of a few advantages. The selection rules, including polarization characteristics, for two-photon absorption (TPA) differ from those for one-photon absorption (OPA) enabling one to obtain additional information about electronic excitations in

nanocrystals. Resonant second-harmonic scattering (RSHS) and/or two-photon-excited resonant luminescence (RL) signals from nanocrystals can be easily obtained in most cases. We note that the second-harmonic generation (SHG) is forbidden in commonly used isotropic host matrices and further the incident light can be completely cut off by an appropriate filter. Since the sample is transparent to the incident photon, a correction of the signals due to reabsorption, which is very important in the detailed analysis of the TPL excitation spectra, also becomes easier compared to one-photon-excitation spectroscopy.

II. EXPERIMENT

We studied two samples of CuCl spherical QD's. The mean radii of the nanocrystals R_0 are 2.4 nm and 2.9 nm, as measured by small-angle x-ray scattering. The plane-parallel plate specimens with a thickness of 0.25 mm were used in the experiments. The corresponding OPA spectra at 2 K are shown in Figs. 2 and 3. The TPL spectra were excited by using a pulsed radiation from a wavelength-tunable Ti-sapphire laser pumped by a Q -switched Nd³⁺:YAG laser (where YAG denotes yttrium aluminum garnet). Twice the energy of the incident photon (from 3.2 to 3.34 eV) swept the entire region of the low-energy confined states of the Z_3 exciton. The linearly polarized laser beam (≈ 0.5 -kW peak power, 50-ns pulse duration, 3-kHz repetition rate, 1-meV spectral width) was focused by a lens with a focal length of 5 cm onto the specimen cooled to 2 K in a helium cryostat. The secondary emission in the quasiforward direction was collected by a set of quartz lenses and dispersed with a single-grating monochromator equipped with a cooled optical multichannel detector. A spectral resolution of 2 meV was adopted. A liquid filter of CuSO₄ saturated solution was used to cut off the fundamental radiation of the Ti-sapphire laser. The TPL intensity was confirmed to be proportional to the squared average power of the incident radiation. However, the power was kept constant by a variable optical density filter during the experiments. Because the optical density of the samples varies significantly in the spectral region investigated, all the TPL spectra were corrected for reabsorption regarding the incident light as a parallel beam; this should be reasonable because the waist length of the focused laser beam is larger than the sample thickness. To extract the respective intensities from the spectra composed of overlapping peaks, a fitting was made in terms of multiple-component Gaussian functions.

III. RESULTS

Figure 1 shows a set of TPL spectra obtained with different incident photon energies for the specimen with a nanocrystal mean size of 2.9 nm. The TPL spectra of the sample with nanocrystals of average size 2.4 nm contain the same lines showing similar behaviors. Due to size distribution of the nanocrystals, each spectrum corresponds to particles of a definite size resonantly excited within the inhomogeneously broadened absorption band of the Z_3 exciton. A relatively narrow peak at $2\hbar\omega_i$, which is just equal to twice the incident photon energy $2E_i = 2\hbar\omega_i$, dominates in both sets of spectra and shows a resonant enhancement when $2E_i$ falls in

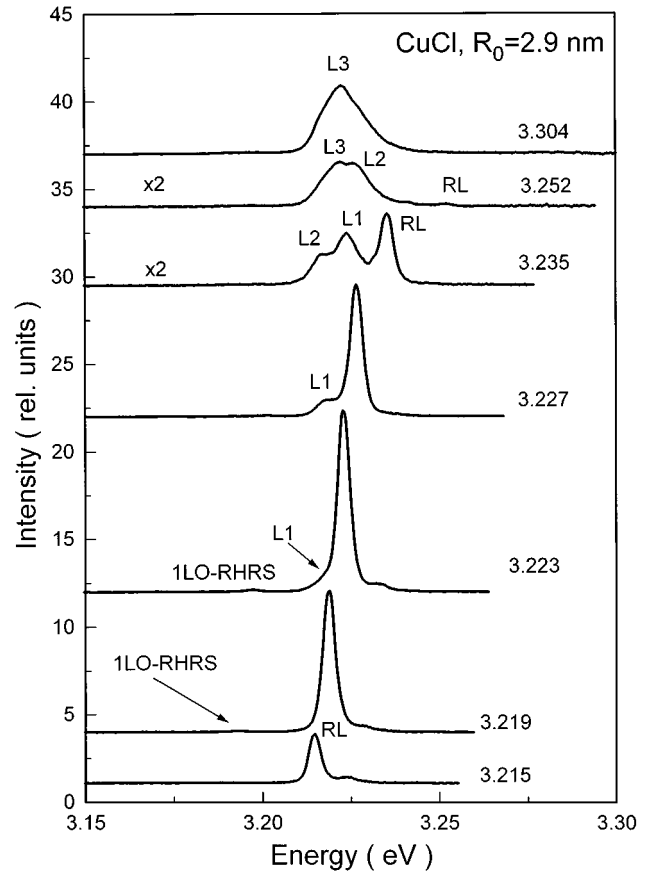


FIG. 1. Two-photon-excited luminescence (TPL) spectra of CuCl dots with $R_0 = 2.9$ nm. Resonant luminescence and three luminescence bands (see the text) are marked by RL and L1, L2, L3, respectively. A weak band of RHRS by LO phonons is also shown. The intensity of two spectra are multiplied by 2. Twice the incident photon energies are indicated.

the region of the OPA peak corresponding to the $1S$ confined state of the Z_3 exciton. This peak corresponds to either the two-photon-excited RL or RSHS, which should, in principle, be distinguished in time-resolved measurements. However, it is outside the scope of the present work. Hereafter we shall refer to it as RL. A weak band of the resonant hyper-Raman scattering (RHRS) by LO phonons with a ‘‘Raman’’ shift of 25.5 meV, corresponding to the CuCl bulk LO-phonon energy,¹⁵ is also clearly observed in the spectra of both samples. The RHRS signal emerges at the same incident photon energies as the RL peak. No signal that may be assigned to the TO phonon was observed. An increase of the incident photon energy results in a consecutive appearance of two strong luminescence bands marked in Fig. 1 as L1 and L2, respectively. Intensities of these bands depend remarkably on E_i . The Stokes shift of these both bands $\Delta L_1(\Delta L_2) = 2\hbar\omega_i - E_{L1(L2)}$ was found to increase with increasing excitation energy, where $E_{L1(L2)}$ is the peak energy of L1(L2) band. A broad band (L3) whose peak energy does not depend on the excitation wavelength appears when $2\hbar\omega_i$ is larger than or ≈ 3.25 eV and dominates the spectra.

To clarify origins of the TPL bands we measured the respective excitation spectra of the RL, L1, L2, and L3 bands of both specimens. They are presented in Figs. 2 and 3,

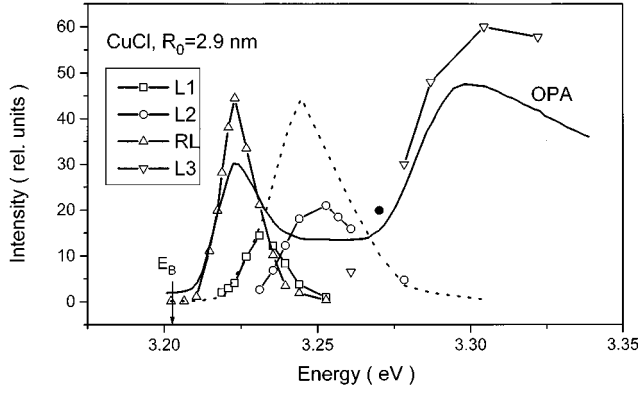


FIG. 2. Excitation profiles of TPL bands and OPA spectrum (solid line) for CuCl dots with $R_0 = 2.9$ nm. Calculated position of the $L2$ excitation spectrum is shown by the dotted curve (see the text). A solid circle corresponds to the sum of the intensities of the $L2$ and $L3$ bands when the band intensities cannot be reliably measured due to coincidence of their peak positions. The arrow shows the exciton energy of bulk CuCl.

where the relevant OPA spectra are also shown for comparison. The main results are summarized as follows: (1) the peak of the RL spectrum coincides exactly with the lowest-energy OPA peak; (2) the maximum of the excitation spectra of the $L1$ band shifts from the corresponding OPA peak by ≈ 8.5 meV and ≈ 10 meV for specimens with $R_0 = 2.9$ nm and 2.4 nm, respectively; (3) the relevant shifts of the $L2$ band are 24 meV and 21.5 meV; and (4) the $L3$ band intensity greatly increases when twice the incident photon energy falls in the region of the higher-energy confined states of Z_3 and $Z_{1,2}$ excitons of CuCl QD's.

In Fig. 4 we represent the Stokes shifts of the $L1$, $L2$, and $L3$ bands as a function of the confinement energy of the $1S$ state $\Delta_{1S} = E_{1S} - E_B \equiv 2\hbar\omega_i - E_B$, where E_{1S} is the energy of the $1S$ state in the quantum dot and $E_B = 3.2022$ eV is the energy of the Z_3 exciton in bulk CuCl.¹⁶ We find that ΔL_1 changes in the ranges $6 < \Delta L_1 < 12.5$ meV and $8 < \Delta L_1 < 14.5$ meV for the samples with $R_0 = 2.9$ nm and 2.4 nm, respectively, and the corresponding variations of ΔL_2 are $16.5 < \Delta L_2 < 25.5$ meV and $20 < \Delta L_2 < 34$ meV.

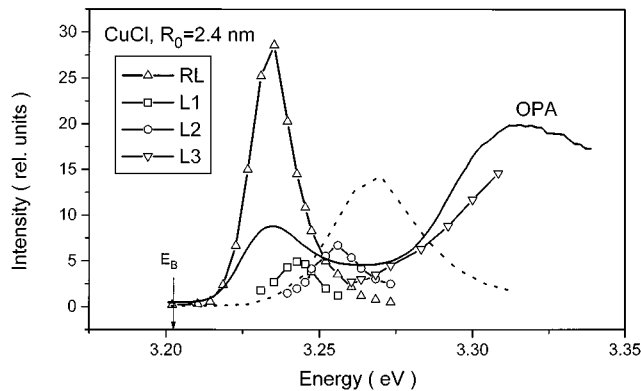


FIG. 3. Same as Fig. 3, but for $R_0 = 2.4$ nm.

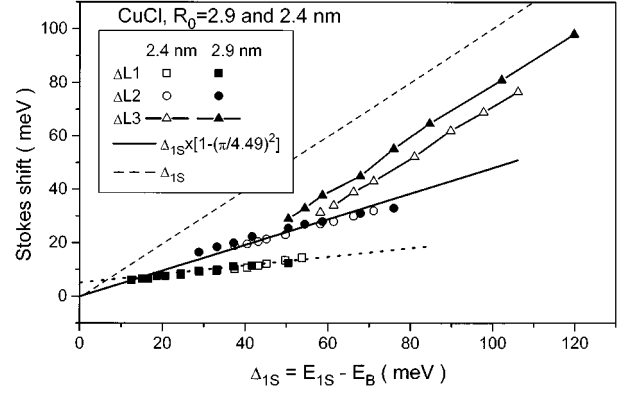


FIG. 4. Stokes shift of the luminescence bands $L1$, $L2$, and $L3$, as a function of the confinement energy Δ_{1S} . The solid line is the calculated dependence for $L2$ (Δ_{1S}). The short-dashed line is a straight line fitted to the result of $\Delta L1(\Delta_{1S})$ (see Fig. 7 for details). The dashed line shows that the $L3$ peak position does not depend on the incident photon energy.

IV. DISCUSSION

As follows from Ref. 17, in the dipole approximation there are two channels of two-photon generation of excitons in quantum dots of semiconductor of T_d symmetry. The first one, in the absence of valence-band mixing, has the selection rules satisfying the relations $\Delta l = l_e - l_h = \pm 1$ and $\Delta m = m_e - m_h = 0, \pm 1$, where $l_{e,h}$ are the angular momenta of the electron and hole and $m_{e,h}$ are their projections. The selection rules differ from those for one-photon transitions: $\Delta n = 0$, $\Delta l = 0$, and $\Delta m = 0$. The second important channel for two-photon generation of excitons has the same selection rules as those for one-photon transitions. This channel describes transitions for which the intermediate states are bands that are different from the conduction and valence bands in question. In this case the matrix element of TPA may be represented as a product of ω -independent constants and quadratic combinations of the Cartesian components of the vector potential. For crystals of T_d symmetry only one such constant Q is nonvanishing.⁶ This Q term is responsible for the SHG process in noncentrosymmetric semiconductors. So the two-photon transition is allowed from the ground state to the $1S$ exciton state due to the second channel, whereas it is allowed to the $1P$ state due to the first channel. On the other hand, the one-photon transition between ground and $1S$ states is allowed, but that between ground and $1P$ states is forbidden. It is not important in the present case that the polarization selection rules are different for the one- and two-photon transitions¹² and for the first and second channels of two-photon generation of excitons¹⁷ since randomly oriented nanocrystal systems are under study.

Since the $L3$ band has a fixed peak energy that is independent of the excitation wavelength (Fig. 4), it is ascribed to a thermalized emission due to recombination of the exciton in QD's at the band edge.¹⁸ For high incident photon energies, the shape of the $L3$ band should reflect more or less the size distribution of QD's because nanocrystals of all sizes can be excited. A detailed study of this behavior is beyond the scope of this paper.

Let us make use of the scheme shown in Fig. 5 for the

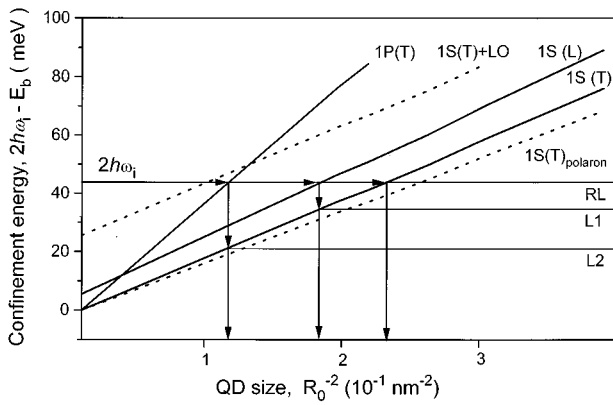


FIG. 5. Schematic of the origin of the RL, L1, and L2 bands resulting from the resonant two-photon excitation of QD's of different sizes. Dotted lines show the energies of the possible 1S exciton polaron and exciton-LO-phonon complex states. *L* and *T* denote the longitudinal and transverse exciton states, respectively (see the text).

size dependence of low-energy confined states of the Z_3 exciton to consider the possible assignments of other bands in the TPL spectra of the spherical CuCl QD's. The narrow peak at $2\hbar\omega_i$ (see, Fig. 1) can be undoubtedly assigned to the signal of two-photon-excited RL or RSHS. It should be noted that both one- and two-photon transitions must be allowed simultaneously for both the RL and RSHS because the two-photon absorption and one-photon luminescence processes are involved in them. Taking into account the above selection rules, we can conclude that only the 1S exciton state of quantum dots may be responsible for the signal. This statement is also supported by the fact that the excitation spectra of RL coincide with the lowest-energy peak of OPA spectra of both samples (Figs. 2 and 3) reflecting the size distribution of the nanocrystals.

It is important to note that in our experiments we could not observe any luminescence band that should be attributed to annihilation of the ground 1S exciton polaron state,¹ shown by the dotted line in Fig. 5. Since a self-trapped exciton or polaron may be mainly excited through a free exciton,¹⁹ the excitation spectrum of the relevant luminescence band must coincide with that of the free exciton that has been observed in Ref. 1. The most likely candidate in this sense is the L1 band, but it shows up in the excitation spectrum at a considerably different energy from both the RL excitation spectrum and OPA peak corresponding to the 1S exciton transition. Consequently, this observation contradicts the behaviors of the exciton polaron. The reason why the annihilation luminescence of the 1S exciton polaron was not observed in the case of two-photon excitation in our samples is not clear to us.

The intensity of RHRS by a LO phonon undergoes an ordinary incoming resonance with the 1S exciton transition.¹³ Accordingly to Fig. 5, the 1S and 1P states belonging to the nanocrystals of different sizes R_{1S} and R_{1P} may be directly excited for a given $2\hbar\omega_i$. Moreover, $R_{1S} < R_{1P}$ holds. It immediately follows that the excitation spectrum of TPL bands resulting from the excitation of the 1P state should be shifted to the high-energy side from that

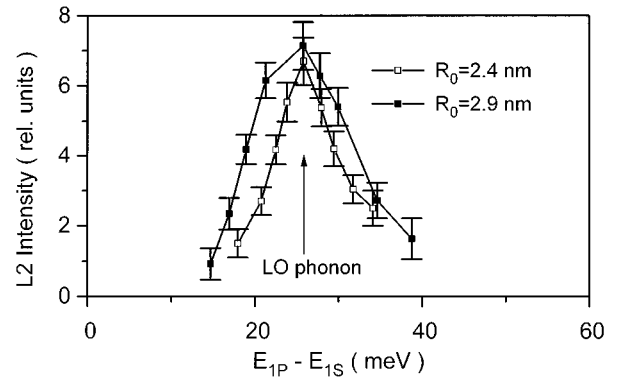


FIG. 6. Intensity of the L2 band as a function of the energy gap between the 1P and 1S states of the *T* exciton, $E_{1P} - E_{1S}$. The LO-phonon energy is shown by an arrow. Solid lines are only a guide to the eyes.

of the RL band since the luminescence intensity must be proportional to the number of nanocrystals. The expected shape of the excitation spectrum can be approximately estimated by using the relation $I_{1P}\{E + \Delta_{1S} \times [(4.49/\pi)^2 - 1]\} \propto I_{1S}(E)$, where $I_{1S}(E) = I_{RL}(E)$ is the observed excitation spectrum of the RL band. The expected spectrum thus estimated is shown by dotted curves in Figs. 2 and 3. The excitation spectrum of the L2 band is consistent with the calculated spectrum. It is reasonable to suppose that the L2 band originates from recombination of the 1S state populated by the relaxation of the 1P state; note that both nonradiative and radiative relaxation is possible because the one-photon transition between these states is allowed. This statement is supported by the fact that the observed Stokes shift (see Fig. 4) is well described by the calculated value using $\Delta L_2 = E_{1S}(R_{1S}) - E_{1S}(R_{1P}) = [E_{1S}(R_{1S}) - E_B][1 - (R_{1S}/R_{1P})^2] = \Delta_{1S}[1 - (\pi/4.49)^2]$, where $E_{1S}(R)$ is the 1S exciton state energy for a QD of radius R . However, there is an evident difference between the L2 excitation spectra and their calculated positions, especially for the sample with $R_0 = 2.4$ nm (see Fig. 3). This discrepancy is considered to arise from the fact that *p*-type LO-phonon-assisted transitions begin to contribute resonantly to the intensity of this band for QD sizes for which $E_{1P} - E_{1S}$ does not differ much from the LO-phonon energy.¹ In Fig. 6, the intensity of the L2 band is plotted as a function of $E_{1P} - E_{1S}$ for both specimens. According to Ref. 1, the confined LO phonons with angular momentum $l=1$, or *p*-type LO phonons, will be involved in this process via the deformation-potential interaction.

Next, we would like to show that the observed behaviors of the L1 band can be unambiguously interpreted in terms of longitudinal and transverse excitons, which we have not taken into account so far. It is well known⁶ that the *L-T* exciton splitting caused by the long-range exchange interaction is described by an equation that is similar to the one that describes the Lydden-Sachs-Teller splitting of LO-TO phonons. Although an adequate description of the *L-T* splitting of excitons in nanocrystals is yet to be developed, it seems reasonable to suppose that the *L-T* exciton splitting exists in QD's because the LO-TO phonon splitting has been observed in QD's based on I-VII compounds.²⁰ Another rea-

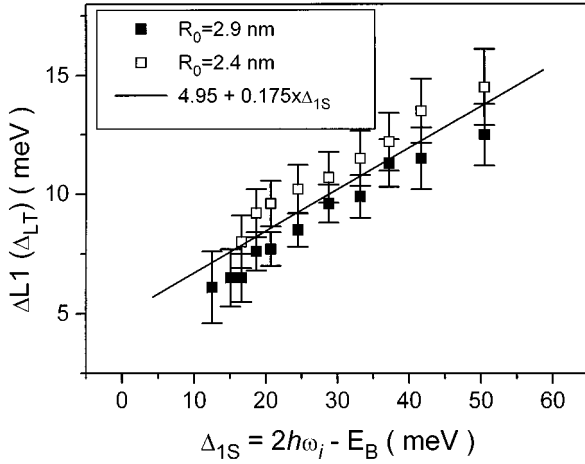


FIG. 7. Stokes shift of the $L1$ band $\Delta L1$ or the L - T exciton splitting energy Δ_{LT} as a function of the incident photon energy $\Delta_{1S} = E_{1S} - E_B = 2\hbar\omega_i - E_B$. The solid line is a result of the fitting of the experimental data by a straight line $\Delta L1 = 4.95 + 0.175 \times \Delta_{1S}$.

son is the fact that in the case of CuCl, the Wannier exciton Bohr radius of 0.7 nm is close to the size of the unit cell (0.541 nm¹⁵) so that, in some sense, the exciton may be considered as a Frenkel exciton.²¹

The L exciton energy should be always higher than that of the T exciton by Δ_{LT} . Three-dimensional confinement in nanocrystals should also cause a size quantization of both the L and T exciton states. We suppose that, analogous to the bulk,²² the two-photon generation of the L exciton is allowed in QD's and one-photon generation is forbidden. Then the $L1$ band arises due to the two-photon generation of the L excitons in the lowest-energy confined state $1S_L$ followed by a subsequent relaxation of the L excitons to the $1S$ state of T excitons $1S_T$ and finally radiative annihilation of the T excitons (Fig. 5). Indeed, the observed shift of the $L1$ band excitation spectra to the higher-energy side of the RL band (Figs. 2 and 3) shows that this band results from photoexcitation to some exciton state with energy higher than the $1S$ state of the T exciton. Other confinement states of the T exciton ($1P$, $1D$, $2S$, etc.) having higher energies cannot be responsible for $L1$. Then the observed Stokes shift $\Delta L1$, shown in detail in Fig. 7, represents a variation of the L - T exciton splitting energy Δ_{LT} as a function of Δ_{1S} . The result reveals that it increases with the decrease of QD size. It is noted that the $L1$ luminescence feature is quite different, in a few aspects, from the luminescence band reported for the CuCl nanocrystals of size range $R \sim 5 - 15$ nm.²³ For the latter, the intensity drastically increases when the energy of the $1S$ confined exciton state coincides with the energy of a surface electromagnetic wave mode (surface exciton) and, more importantly, the energy position is independent of the nanocrystal size. In our case the experimental size dependence of $\Delta L1$ may be well fitted by a straight line $\Delta L1 = 4.95 + 0.175 \Delta_{1S}$, which yields an L - T exciton splitting energy of 4.95 meV at $\Delta_{1S} = 0$. This value agrees nicely with the CuCl bulk value of 5.0–5.7 meV.¹⁵ From the observed relation an effective translational mass of the L exci-

ton $m_{LE} = (0.77 \pm 0.7)m_{TE}$, where m_{TE} is the effective translational mass of the T exciton, can be easily evaluated by supposing the same functional size dependence for both the L and T $1S$ excitons in QD's. The value thus obtained differs significantly from the bulk value of $1.35m_{TE}$ measured by hyper-Raman scattering experiment.²⁴ This fact, as well as the size dependence of Δ_{LT} , is not necessarily unexpected. As a matter of fact, in bulk CuCl the observed exciton L - T splitting²⁵ can be expressed in terms of the relation $\Delta_{LT}(\mathbf{K}) = \Delta_{LT}(0) + \alpha \hbar^2 \mathbf{K}^2 / 2m_0$ for small $\mathbf{K} < 6 \times 10^6$ cm⁻¹, where \mathbf{K} is the exciton wave vector; $\Delta_{LT}(0) = 5.7$ meV; $\alpha = m_0(1/M_L - 1/M_T) = -0.12$; m_0 , M_L , and M_T are the free-electron mass and effective masses of the L and T excitons. This equation does not hold for $\mathbf{K} > 6 \times 10^6$ cm⁻¹ since in the region $\mathbf{K} \sim 10^7$ cm⁻¹ the exciton branches should cross each other. However, it is not possible, in principle from a physical point of view. Obviously, the constant α should change sign in the region $\mathbf{K} > 10^7$ cm⁻¹, i.e., the effective mass of the L exciton should be smaller than that of the T exciton. Three-dimensional confinement should cause size quantization of both exciton branches. The wave vector of the $1S$ confined exciton in QD, whose radius is smaller than $\pi 10^{-7}$ (cm) = 3.14 nm, is larger than 10^7 cm⁻¹. Then, to describe the exciton L - T splitting for specimens under study we can use the equation $\Delta_{LT}(R) = \tilde{\Delta}_{LT}(R) + \alpha \hbar^2 \xi_{nl}^2 / 2m_0 R^2$ with $\alpha > 0$, where ξ_{nl} is the n th root of the l th-order spherical Bessel function $j_l(\xi_{nl}) = 0$. A rough estimation according to Ref. 6 shows that the value of $\tilde{\Delta}_{LT}(R)$ is practically independent of the QD radius R in the weak confinement regime. This means that the size dependence of the exciton L - T splitting is determined by the size quantization of the exciton branches, i.e., by $\alpha \hbar^2 \xi_{nl}^2 / 2m_0 R^2$. The effective mass of the L exciton thus obtained reflects a nonparabolicity of the L exciton band far from the Γ point in the Brillouin zone.

V. CONCLUSION

We have analyzed the low-temperature luminescence spectra resulting from a size-selective two-photon excitation of the low-energy confined Z_3 -exciton states in CuCl spherical nanocrystals of different sizes embedded in a glass matrix. It has been found that the spectra contain at least five bands with different spectral behaviors. One of them is attributed to the RHRS by LO phonons with an energy of 25.5 meV. Excitation spectra of the other TPL bands and size dependences of the band energies show that they arise due to annihilation of the exciton in the lowest-energy state excited both directly and through the high-energy confined states. We have shown that the fine structure of the TPL in CuCl nanocrystals can be unambiguously interpreted in terms of longitudinal and transverse exciton confined states and resonant enhancement of phonon-assisted luminescence when the energy gap between $1S$ and $1P$ states of the T exciton is close to the LO-phonon energy. It has been shown that in accordance with theoretical prediction,¹⁷ there are two channels of two-photon generation of excitons in CuCl QD's. One of them, determined by the Q term, governs the RL or/and RSHS processes involving the lowest-energy confined state of the T exciton $1S_T$ and causes the direct two-photon

excitation of L excitons in the $1S_L$ state. Another channel with selection rules different from those for the one-photon transitions is responsible for creation of excitons in the $1P_T$ state, which results in subsequent LO-phonon-mediated transition to the $1S_T$ exciton state and radiative annihilation of the latter. We have observed the size dependence of the long-range exchange interaction Δ_{LT} , which is supposed to be caused by a nonparabolicity of the L exciton band far from the center of the Brillouin zone.

ACKNOWLEDGMENTS

The authors are grateful to Professor K. Sakoda for the measurement of the OPA spectra at 2 K, Dr. A. Yamanaka and A. Itoh for their help in the experiment, and Dr. V. V. Golubkov for SAXS measurements. A.V.F. is grateful to the Japan Society for the Promotion of Science and the Russian Basic Research Foundation, Grants Nos. 96-02-16235a, 96-02-16242a, and 95-02-03821a, for financial support during this work.

*Permanent address: S. I. Vavilov State Optical Institute, 199034 St. Petersburg, Russia.

¹T. Itoh, M. Nishijima, A. I. Ekimov, C. Gourdon, Al. L. Efros, and M. Rosen, *Phys. Rev. Lett.* **74**, 1645 (1995).

²K. Inoue, A. Yamanaka, K. Toba, A. V. Baranov, A. A. Onushchenko, and A. V. Fedorov, *Phys. Rev. B* **54**, 8321 (1996).

³T. Takagahara, *Phys. Rev. B* **47**, 4569 (1993).

⁴M. A. Chamarro, C. Gordon, P. Lavallard, and A. I. Ekimov, *Jpn. J. Appl. Phys. Suppl.* **34-1**, 12 (1995).

⁵M. Nirmal, D. J. Norris, M. Kuno, M. G. Bawendi, Al. L. Efros, and M. Rosen, *Phys. Rev. Lett.* **75**, 3728 (1995).

⁶G. L. Bir and G. E. Pikus, *Symmetry and Strain-Induced Effects in Semiconductors* (Keter, Jerusalem, 1974).

⁷U. Woggon, F. Gindele, O. Wind, and C. Klingshirn, *Phys. Rev. B* **54**, 1506 (1996).

⁸D. Fröhlich, E. Mohler, and C. Uihlein, *Phys. Status Solidi B* **55**, 175 (1973).

⁹T. Itoh, Y. Iwabuchi, and T. Kirihara, *Phys. Status Solidi B* **146**, 531 (1988).

¹⁰A. I. Ekimov, A. A. Onushchenko, A. G. Plyukhin, and Al. L. Efros, *Zh. Éksp. Teor. Fiz.* **88**, 1490 (1985) [*Sov. Phys. JETP* **88**, 891 (1985)].

¹¹Al. L. Efros and A. L. Efros, *Fiz. Tekh. Poluprovodn.* **16**, 1209 (1982) [*Sov. Phys. Semicond.* **16**, 772 (1982)].

¹²D. Fröhlich, M. Haselhoff, K. Reinmann, and T. Itoh, *Solid State Commun.* **94**, 189 (1995).

¹³A. V. Baranov, K. Inoue, K. Toba, A. Yamanaka, V. I. Petrov, and A. V. Fedorov, *Phys. Rev. B* **53**, 1721 (1996).

¹⁴M. E. Schmidt, S. A. Blanton, M. A. Hines, and P. Guyot-Sionnest, *Phys. Rev. B* **53**, 12 629 (1996).

¹⁵*Semiconductors*, edited by O. Madelung, M. Schultz, and H. Weiss, Landolt-Börnstein, New Series, Group III, Vol. 17, Pt. a (Springer, Berlin, 1982).

¹⁶K. Saito, M. Hasuo, T. Hatano, and N. Nagasawa, *Solid State Commun.* **94**, 33 (1995).

¹⁷A. V. Fedorov, A. V. Baranov, and K. Inoue, *Phys. Rev. B* **54**, 8627 (1996).

¹⁸A. I. Ekimov, I. A. Kudryavtsev, M. G. Ivanov, and A. L. Efros, *J. Lumin.* **46**, 83 (1990).

¹⁹E. I. Rashba, in *Excitons*, edited by E. I. Rashba and M. D. Sturge (North-Holland, Amsterdam, 1982), p. 543.

²⁰A. V. Fedorov, A. V. Baranov, and K. Inoue (unpublished).

²¹R. S. Knox, *Theory of Excitons* (Academic, New York, 1963).

²²M. M. Denisov and V. P. Makarov, *J. Phys. C* **5**, 2651 (1972).

²³A. I. Ekimov, A. A. Onushchenko, M. E. Raikh, and Al. L. Efros, *Zh. Éksp. Teor. Fiz.* **90**, 1795 (1986) [*Sov. Phys. JETP* **63**, 1054 (1986)].

²⁴T. Mita, K. Sotome, and M. Ueta, *J. Phys. Soc. Jpn.* **48**, 486 (1980); *Solid State Commun.* **33**, 1135 (1980).

²⁵Y. Onodera, *J. Phys. Soc. Jpn.* **49**, 1845 (1980).